Глушак Степан Петрович
Калюжний Юрій Володимирович

Фазова рівновага ланцюгової рідини юкавівських твердих сфер, полідисперсної за довжиною ланцюга: Димерна термодинамічна теорія збурень

Роботу отримано 10 квітня 2008 р.

Затверджено до друку Вченою радою ІФКС НАН України

Рекомендовано до друку відділом теорії нерівноважних процесів

Виготовлено при ІФКС НАН України

Національна академія наук України

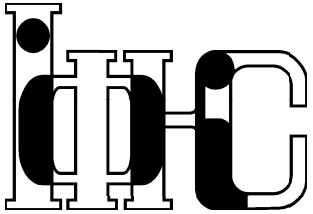

ІНСТИТУТ ФІЗИКИ КОНДЕНСОВАНИХ СИСТЕМ

ICMP–08–08E

S.P. Hlushak and Yu.V. Kalyuzhnyi

PHASE COEXISTENCE IN THE HARD-SPHERE YUKAWA CHAIN FLUID WITH CHAIN LENGTH POLYDISPERSITY: DIMER THERMODYNAMIC PERTURBATION THEORY

ЛЬВІВ

УДК: 532; 532.74; 532.772; 544.023.522

PACS: 05.70.Ce; 61.20.Gy; 64.75.Va; 83.80.Rs

Фазова рівновага ланцюгової рідини юкавівських твердих сфер, полідисперсної за довжиною ланцюга: Димерна термодинамічна теорія збурень

С.П. Глушак, Ю.В. Калюжний

Анотація. В рамках димерної термодинамічної теорії збурень Вертхейма, досліджено фазову поведінку ланцюгової рідини юкавівських твердих сфер полідисперсної за довжиною ланцюга. Структурні та термодинамічні властивості базисної системи юкавівських димерів описані у полімерному середньосферичному наближенні. Аналітичні вирази для надлишкової вільної енергії Гельмгольца, хімічних потенціалів та тиску виражаються двома моментами функції розподілу довжин ланцюгів. Це дозволило порахувати повну фазову діаграму рідина-газ (критичні бінодалі, криві тіні та хмари) та функції розподілу співіснуючих фаз.

Phase coexistence in the hard-sphere Yukawa chain fluid with chain length polydispersity: Dimer thermodynamic perturbation theory

S.P. Hlushak, Yu.V. Kalyuzhnyi

Abstract. An extension of the dimer version of Wertheim's thermodynamic perturbation theory is proposed and used to treat polydisperse mixture of the hard-sphere Yukawa chain fluid with chain length polydispersity. The structure and thermodynamic properties of the reference system of Yukawa hard-sphere dimers, are described using polymer mean spherical approximation. Analytical expressions for the Helmholtz free energy, chemical potential and pressure in terms of the two chain length distribution function moments are derived. Full liquid-gas phase diagram, including critical binodal, cloud and shadow curves and distribution functions of the coexisting phases were calculated.

Подається в Journal of Chemical Physics
Submitted to Journal of Chemical Physics

1. Introduction

This is our second paper on the thermodynamic properties and phase behaviour of the polydisperse hard-sphere Yukawa chain mixture. In the previous paper [1] the mixture was studied using high temperature approximation based on the recently derived analytical expression for the Laplace transform of the site-site radial distribution function for the polydisperse hard-sphere chain fluid [2].

Thermodynamic properties of the monodisperse hard-sphere Yukawa chain fluid were studied recently using statistical associating fluid theory for the potentials of variable range (SAFT-VR) [3]. The theory is based on Wertheim's first-order thermodynamic perturbation theory (TPT1) of polymerization [4, 5] with the reference system represented by the Yukawa hard-sphere fluid. Later the structure and thermodynamical properties of the monodisperse Yukawa hard-sphere chain fluid were investigated using first-order liquid state perturbation theory [6], polymer mean spherical approximation (PMSA) [7–10] and dimer version of the thermodynamic perturbation theory (TPTD) [10]. In the firs-order perturbation theory of Wang and Chiew [6], which appears to be equivalent to the HTA utilized in our previous study [1], the perturbation integral was decomposed and coefficients of the corresponding series were calculated numerically using integral equation theory of Chiew [11]. The PMSA corresponds to the MSA version of the product-reactant Ornstein-Zernike approach (PROZA) [12–16], which in turn originates from the multidensity integral-equation theory for associating fluids developed by Wertheim [4,17]. TPTD was originally developed by Ghonasgi and Chapman [18] and independently by Chang and Sandler [19]. The concept of the theory is similar to that of Wertheim's TPT1 [5] with the reference system represented by the fluid of dimers. In the previous study [10] thermodynamical properties and contact value of the site-site radial distribution function (RDF) for the reference system of Yukawa dimers were obtained in the frames of the PMSA

In this paper we extend TPTD to treat polydisperse mixture of Yukawa hard-sphere chains. The theory is used to study the liquid-gas phase behavior of the mixture with chain length polydispersity. The paper is organized as follows: In Sec. II we present the model and in Sec. III we discuss details of the TPTD. Closed form analytical expressions for the thermodynamic properties and contact value of the site-site RDF of the reference system are derived in Sec. IV and in Sec. V we present and discuss our results for the phase behavior of the model. Our conclusions are collected in Sec. VI.

2. The model

We consider a multi-component mixture of freely-jointed tangent hard-sphere Yukawa chain molecules with a total number density $\rho = N/V$. The molecules of species m with a number density $\rho_m = N_m/V$ are represented by m tangentially bonded hard-sphere Yukawa monomers of equal hard-core diameter σ. The system is characterized by the chain length distribution function $f(m) = \rho_m/\rho$. Here

$$\rho = \sum_m \rho_m. \tag{2.1}$$

Nonbonded monomers, regardless of whether they belong to the same molecule or to the different molecules, interact directly via the hard-sphere potential $\Phi^{(hs)}(r)$ and Yukawa potential $\Phi^{(Y)}(r)$,

$$\Phi(r) = \Phi^{(hs)}(r) + \Phi^{(Y)}(r), \tag{2.2}$$

where

$$\beta\Phi^{(Y)}(r) = -\frac{K}{r}e^{-zr}, \tag{2.3}$$

$\beta = 1/kT$ and r is the center-to-center separation between the two monomer beads.

3. TPTD

According to the TPTD Helmholtz free energy of the multi-component chain fluid $A^{(TPTD)}$ can be written in the following form:

$$\beta\frac{A^{(TPTD)}}{V} = \beta\frac{A^{(id)}}{V} + \beta\frac{\Delta A^{(ref)}_{dim}}{V} - \ln g_{dim}(\sigma)\left(\frac{1}{2}\rho_{mon} - \rho\right), \tag{3.1}$$

where $A^{(id)}$ is the ideal gas contribution to the Helmholtz free energy, $\Delta A^{(ref)}_{dim}$ denotes the excess Helmholtz free energy of the reference system, represented by the fluid of Yukawa hard-sphere dimers, $g_{dim}(\sigma)$ is the site-site RDF of Yukawa dimers at the contact and ρ_{mon} represents the monomer density of the system, i.e.

$$\rho_{mon} = \sum_m m\rho_m. \tag{3.2}$$

Thus TPTD yields Helmholtz free energy of the chain fluid (3.1) provided that thermodynamic and structure properties of the reference system are given. Expressions for the chemical potential and pressure follows from (3.1):

$$\begin{aligned}\beta\mu_m^{(TPTD)} &= \beta\mu_m^{(id)} + \frac{1}{2}m\beta\Delta\mu_{dim}^{(ref)} - m\frac{\partial \ln g_{dim}(\sigma)}{\partial\rho_{mon}}\left(\frac{1}{2}\rho_{mon} - \rho\right)\\ &\quad - \ln g_{dim}(\sigma)\left(\frac{1}{2}m - 1\right),\end{aligned} \tag{3.3}$$

$$\beta P^{(TPTD)} = \beta P^{(ref)}_{dim} - \left(\frac{1}{2}\rho_{mon} - \rho\right)\left(1 + \rho_{mon}\frac{\partial \ln g_{dim}(\sigma)}{\partial\rho_{mon}}\right), \tag{3.4}$$

where $\mu_m^{(id)}$ is the ideal gas chemical potential, $\Delta\mu_{dim}^{(ref)}$ is the excess chemical potential of the reference system and $P_{dim}^{(ref)}$ is the reference system pressure.

4. Reference system properties

In this study the properties of the reference system, represented by the Yukawa hard-sphere dimer fluid with the number density $\rho_{dim} = \rho_{mon}/2$ are described using two-density theory for the site-site interaction [17, 20, 21]. For the Yukawa hard-sphere dimer fluid the theory consists of the Ornstein-Zernike equation

$$\hat{\mathbf{h}}(k) = \hat{\mathbf{c}}(k) + \rho_{mon}\hat{\mathbf{c}}(k)\boldsymbol{\alpha}\hat{\mathbf{h}}(k), \tag{4.1}$$

supplemented by the polymer MSA (PMSA) closure conditions

$$\mathbf{c}(r) = \mathbf{E}\frac{K}{r}e^{-zr}, \qquad r > \sigma \tag{4.2}$$

$$\mathbf{h}(r) = -\mathbf{E} + (\mathbf{1} - \mathbf{E})\frac{\delta(r-\sigma)}{4\pi\sigma^2\rho_{mon}}, \qquad r < \sigma. \tag{4.3}$$

Here $\hat{\mathbf{h}}(k)$, $\hat{\mathbf{c}}(k)$, $\mathbf{1}$, $\boldsymbol{\alpha}$ and $\mathbf{E}$ are the following matrices:

$$\hat{\mathbf{h}}(k) = \begin{pmatrix}\hat{h}_{00}(k) & \hat{h}_{01}(k)\\ \hat{h}_{10}(k) & \hat{h}_{11}(k)\end{pmatrix}, \qquad \hat{\mathbf{c}}_{ij}(k) = \begin{pmatrix}\hat{c}_{00}(k) & \hat{c}_{01}(k)\\ \hat{c}_{10}(k) & \hat{c}_{11}(k)\end{pmatrix},$$

$$\mathbf{1} = \begin{pmatrix}1 & 0\\ 0 & 1\end{pmatrix}, \qquad \boldsymbol{\alpha}_i = \begin{pmatrix}1 & 1\\ 1 & 0\end{pmatrix}, \qquad \mathbf{E} = \begin{pmatrix}1 & 0\\ 0 & 0\end{pmatrix},$$

where the matrix components $\hat{h}_{\alpha\beta}(k)$ and $\hat{c}_{\alpha\beta}(k)$ are Fourier transforms of the total $h_{\alpha\beta}(r)$ and direct $c_{\alpha\beta}(r)$ correlation functions, respectively.

Here the lower indices α and β denote the bonding state of the corresponding particle and take the values 0 (non bonded) and 1 (bonded). The relation between the site-site radial distribution function $g_{dim}(r)$ and the partial radial distribution functions is

$$g_{\alpha\beta}(r) = h_{\alpha\beta}(r) + \delta_{0\alpha}\delta_{0\beta} \text{ and } g_{dim}(r) = \sum_{\alpha\beta} g_{\alpha\beta}(r). \qquad (4.4)$$

The PMSA theory discussed above represents a particular case of more general associative MSA (AMSA) theory for associative fluids [22,23] in the complete association limit (CAL) [21]. The solution of the AMSA has been derived earlier for the general case of a multi-component mixture of Yukawa dimerizing hard-sphere fluid [24,25]. Recently this solution was used to derive explicit analytical expressions for the thermodynamical properties of the model in question [25, 26]. For this reason we omit the details of derivation here and only present the final expressions relevant to our model, i.e. one-component dimerizing Yukawa hard-sphere fluid in the CAL. The solution of the AMSA can be reduced to the solution of one single nonlinear algebraic equation for the scaling parameter Γ as introduced by Ginoza [27]. For our model the equation for Γ takes the following form:

$$\Gamma^2 + z\Gamma + \pi K X_0^2 \left(1 + \frac{2\Delta\xi}{\pi\sigma^2}\right)\rho_{mon} = 0 \qquad (4.5)$$

where $\Delta = 1 - \pi\rho_{mon}\sigma^3/6$ and

$$X_0 = -\lambda - \Delta_1\eta - \frac{2\Delta\eta^B}{\pi}\xi. \qquad (4.6)$$

The other quantities are

$$\lambda = -\frac{e^{-\frac{1}{2}z\sigma}}{1+\varphi_0(z\sigma)\sigma\Gamma}, \qquad \eta = \frac{\sigma^3 z^2\phi_1(z\sigma)}{1+\varphi_0(z\sigma)\sigma\Gamma}, \qquad \xi = \frac{\pi}{2\Delta}\frac{\sigma^2\varphi_0(z\sigma)}{1+\varphi_0(z\sigma)\sigma\Gamma},$$

$$\eta^B = \frac{-\frac{\pi}{\Delta}\Theta^\eta\Omega^\lambda + \Theta^\lambda\left(\frac{1}{2}z^2 + \frac{\pi}{\Delta}\Omega^\eta\right)}{\Theta^\eta\left(2\Gamma + \frac{\pi}{\Delta}\rho_{mon}\sigma^2 + z + 2\Omega^\xi\right) + \frac{\Delta}{\pi}\left(z^2 + \frac{2\pi}{\Delta}\Omega^\eta\right)\left(1-\Theta^\xi\right)}, \qquad (4.7)$$

$$\Delta_1 = \frac{2\Omega^\lambda\left(\Theta^\xi - 1\right) - \left[2\Gamma + \frac{\pi}{\Delta}\rho_{mon}\sigma^2 + z + 2\Omega^\xi\right]\Theta^\lambda}{\Theta^\eta\left(2\Gamma + \frac{\pi}{\Delta}\rho_{mon}\sigma^2 + z + 2\Omega^\xi\right) + \frac{\Delta}{\pi}\left(z^2 + \frac{2\pi}{\Delta}\Omega^\eta\right)\left(1-\Theta^\xi\right)}, \qquad (4.8)$$

where

$$\Omega^y = -y\left(\frac{\Delta\xi}{\pi\sigma^2} + \frac{1}{2}\right)\rho_{mon}, \quad \Theta^y = -\sigma y\left(\frac{\Delta\xi}{\pi\sigma^2} + 1\right)\rho_{mon}. \qquad (4.9)$$

Here y represents ξ, η or λ, and

$$\varphi_0(x) = \frac{1-e^{-x}}{x}, \quad \varphi_1(x) = \frac{1-x-e^{-x}}{x^2},$$
$$\phi_1(x) = \frac{1}{x^3}\left[1 - \frac{1}{2}x - \left(1 + \frac{1}{2}x\right)e^{-x}\right].$$

The Γ formalism, used above to solve the set of the PMSA equations (4.1)-(4.3), provides closed expressions for the structure and thermodynamic properties of the system. For the reference system Helmholtz free energy we have:

$$\beta\Delta A_{dim}^{(ref)} = \beta\Delta A^{(hs)} + \beta\Delta A^{(PMSA)}, \qquad (4.10)$$

where Carnahan-Starling expression [28] was chosen to represent the hard sphere contribution

$$\beta\frac{\Delta A^{(hs)}}{V} = \frac{\pi\rho_{mon}^2\sigma^3}{2\Delta}\left(1 + \frac{1}{3\Delta}\right) \qquad (4.11)$$

and $\Delta A^{(PMSA)}$ represent contributions from the Yukawa interaction and dimerization and calculated [25,26] using PMSA theory

$$\beta\frac{\Delta A^{(PMSA)}}{V} = \beta\frac{\Delta E^{(PMSA)}}{V} + \frac{1}{\pi}\left[\frac{(\Gamma)^3}{3} + z\frac{(\Gamma)^2}{2}\right] + \beta\frac{\Delta A^{MAL}}{V} + \frac{K\rho_{mon}}{2\sigma}X_0^2. \qquad (4.12)$$

Here

$$\beta\frac{\Delta A^{MAL}}{V} = -\frac{\rho_{mon}}{2}\ln g_{hs}^{(CS)}(\sigma) - \frac{K\rho_{mon}}{2\sigma}X_0^2 \qquad (4.13)$$

is the mass action law contribution to the free energy and

$$\beta\frac{\Delta E^{(PMSA)}}{V} = -K\rho_{mon}\frac{e^{-z\alpha/2}}{\sigma\varphi_0(z\sigma)}\left[X_0\left(1 + \frac{\Delta\xi}{\pi\sigma^2}\right) - \sigma\Delta_1 - e^{-z\sigma/2}\right] \qquad (4.14)$$

is the contribution to the internal energy due to the Yukawa interaction. In (4.13) $g_{hs}^{(CS)}(\sigma)$ is the Carnahan-Starling expression for the contact value of the RDF for the fluid of hard spheres

$$g_{hs}^{(CS)}(\sigma) = \frac{1}{\Delta} + \frac{\pi\rho_{mon}\sigma^3}{4\Delta^2} + \frac{\pi^2\rho_{mon}^2\sigma^6}{72\Delta^3}. \qquad (4.15)$$

Chemical potential of the reference system is obtained differentiating the free energy (4.10) with respect to the dimer density $\rho_{dim} = \rho_{mon}/2$. We have:

$$\beta\Delta\mu_{dim}^{(ref)} = 2\beta\Delta\mu^{(hs)} + \beta\Delta\mu_{dim}^{(PMSA)}, \qquad (4.16)$$

where

$$\beta\Delta\mu^{(hs)} = \frac{\pi\rho_{mon}\sigma^3}{\Delta}\left(1+\frac{1}{3\Delta}\right)+\frac{\pi^2\rho_{mon}^2\sigma^6}{12\Delta^2}\left(1+\frac{2}{3\Delta}\right) \quad (4.17)$$

$$\beta\Delta\mu_{dim}^{(PMSA)} = -\ln g_{hs}^{(CS)}(\sigma)-\rho_{mon}\frac{\partial \ln g_{hs}^{(CS)}(\sigma)}{\partial\rho_{mon}} + \beta\left[\frac{\partial\left(\Delta E^{(PMSA)}/V\right)}{\partial\rho_{mon}}\right]_{\Gamma\beta}, \quad (4.18)$$

$$\frac{\partial g_{hs}^{(CS)}(\sigma)}{\partial\rho_{mon}} = \frac{5\pi\sigma^3}{12\Delta^2}+\frac{\pi^2\rho_{mon}\sigma^6}{9\Delta^3}+\frac{\pi^3\rho_{mon}^2\sigma^9}{144\Delta^4}. \quad (4.19)$$

The internal energy derivative, which appears in above expression, reads

$$\beta\left[\frac{\partial\left(\Delta E^{(PMSA)}/V\right)}{\partial\rho_{mon}}\right]_{\Gamma\beta} = -K\frac{e^{-\frac{z\sigma}{2}}}{\sigma\varphi_0(z\sigma)}\left[X_0+\frac{\Delta\xi}{\pi\sigma^2}X_0 -\sigma\Delta_1-e^{-\frac{z\sigma}{2}}\right]-K\frac{\rho_{mon}e^{-\frac{z\sigma}{2}}}{\sigma\varphi_0(z\sigma)}\left[\left[\frac{\partial X_0}{\partial\rho_{mon}}\right]_{\Gamma\beta}\left(1+\frac{\Delta\xi}{\pi\sigma^2}\right) -\sigma\left[\frac{\partial\Delta_1}{\partial\rho_{mon}}\right]_{\Gamma\beta}\right], \quad (4.20)$$

where $\left[\frac{\partial X_0}{\partial\rho_{mon}}\right]_{\Gamma\beta}$ is

$$\left[\frac{\partial X_0}{\partial\rho_{mon}}\right]_{\Gamma\beta} = -\eta\left[\frac{\partial\Delta_1}{\partial\rho_{mon}}\right]_{\Gamma\beta}-\frac{2\Delta\xi}{\pi}\left[\frac{\partial\eta^B}{\partial\rho_{mon}}\right]_{\Gamma\beta}, \quad (4.21)$$

and expressions for $\left[\frac{\partial\Delta_1}{\partial\rho_{mon}}\right]_{\Gamma\beta}$ and $\left[\frac{\partial\eta^B}{\partial\rho_{mon}}\right]_{\Gamma\beta}$ are given in the Appendix.

Finally, for the reference system pressure we have:

$$\beta P_{dim}^{(ref)} = \beta P^{(hs)}+\beta\Delta P^{(PMSA)}, \quad (4.22)$$

where

$$\beta P^{(hs)} = \frac{1}{\Delta}\left\{\rho_{mon}+\frac{\pi\rho_{mon}^2\sigma^3}{2\Delta}+\frac{\pi^2\rho_{mon}^3\sigma^6}{12\Delta^2}+\frac{\pi^3\rho_{mon}^4\sigma^9}{216\Delta^2}\right\} \quad (4.23)$$

is the pressure of the hard-sphere fluid and

$$\beta\Delta P^{(PMSA)} = -\frac{\rho_{mon}}{2}\left[\rho_{mon}\frac{\partial\ln g_{hs}^{(CS)}(\sigma)}{\partial\rho_{mon}}+1\right] -\frac{1}{\pi}\left[\frac{(\Gamma)^3}{3}+z\frac{(\Gamma)^2}{2}\right]+\rho_{mon}\beta\frac{\partial\left(\Delta E^{(PMSA)}/V\right)}{\partial\rho_{mon}}-\beta\frac{\Delta E^{(PMSA)}}{V}, \quad (4.24)$$

represent contributions due to the Yukawa interaction and due to the dimerization. It is straightforward to show that

$$\rho_{mon}\beta\frac{\partial\left(\Delta E^{(PMSA)}/V\right)}{\partial\rho_{mon}}-\beta\frac{\Delta E^{(PMSA)}}{V}= = -K\frac{\rho_{mon}^2e^{-\frac{z\sigma}{2}}}{\sigma\varphi_0(z\sigma)}\left[\left(1+\frac{\Delta\xi}{\pi\sigma^2}\right)\left[\frac{\partial X_0}{\partial\rho_{mon}}\right]_{\Gamma\beta}-\sigma\left[\frac{\partial\Delta_1}{\partial\rho_{mon}}\right]_{\Gamma\beta}\right]. \quad (4.25)$$

TPTD expressions for Helmholtz free energy (3.1), chemical potential (3.3) and pressure(3.4) involve the contact value of the Yukawa dimer site-site RDF $g_{dim}(\sigma)$. Following the earlier study [10] we will use here extension of the approximation, suggested by Høye and Stell [29]. We have [10, 25, 26]

$$g_{dim}(\sigma) = g_{dim}^{(hs)}(\sigma)+Kg_{hs}^{(PY)}(\sigma)\frac{X_0^2}{\sigma}\left(1+\frac{\Delta\xi}{\pi\sigma^2}\right)^2 + \frac{1}{2}\left(\frac{K}{\sigma}\right)^2X_0^4\left(1+\frac{2\Delta\xi}{\pi\sigma^2}\right)^2-\frac{K}{2\Delta}\frac{X_0^2}{\sigma}\left(1+\frac{\Delta\xi}{\pi\sigma^2}\right) \quad (4.26)$$

where for the hard-sphere dimer site-site RDF $g_{dim}^{(hs)}(\sigma)$ we have used expression of Ghonasgi and Chapman [18]

$$g_{dim}^{(hs)}(\sigma) = \frac{1+\pi\rho_{mon}/3+C_2\left(\pi\rho_{mon}/6\right)^{C_3}}{2\Delta^2}. \quad (4.27)$$

Here $C_2 = 26.45031$, $C_3 = 6.17$, and $g_{hs}^{(PY)}(\sigma)$ is Percus-Yevick expression for the hard-sphere RDF at the contact, i.e.

$$g_{hs}^{(PY)}(\sigma) = \frac{1}{\Delta}+\frac{\pi\rho_{mon}\sigma^3}{4\Delta^2}. \quad (4.28)$$

To calculate the full chemical potential (3.3), we require $\frac{\partial g_{dim}}{\partial\rho_{mon}}$ derivative, which is given by

$$\frac{\partial g_{dim}(\sigma)}{\partial\rho_{mon}} = \frac{\partial g_{dim}^{(hs)}(\sigma)}{\partial\rho_{mon}}+K\frac{\partial g_{hs}(\sigma)}{\partial\rho_{mon}}\frac{X_0^2}{\sigma}\left(1+\frac{\Delta\xi}{\pi\sigma^2}\right)^2 +\frac{2Kg_{hs}(\sigma)}{\sigma}X_0\left(1+\frac{\Delta\xi}{\pi\sigma^2}\right)\left[\left[\frac{\partial X_0}{\partial\rho_{mon}}\right]_\beta\left(1+\frac{\Delta\xi}{\pi\sigma^2}\right) -\frac{2X_0}{\sigma^3}\left(\frac{\Delta\xi}{\pi}\right)^2\left[\frac{\partial\Gamma}{\partial\rho_{mon}}\right]_\beta\right]-\frac{K\pi\sigma^2m}{16\Delta^2}X_0^2\left(1+\frac{\Delta\xi}{\pi\sigma^2}\right) -\frac{KX_0}{\Delta\sigma}\left[\left[\frac{\partial X_0}{\partial\rho_{mon}}\right]_\beta\left(1+\frac{\Delta\xi}{\pi\sigma^2}\right)-\frac{X_0}{\sigma^3}\left(\frac{\Delta\xi}{\pi}\right)^2\left[\frac{\partial\Gamma}{\partial\rho_{mon}}\right]_\beta\right], \quad (4.29)$$

where $\left[\frac{\partial X_0}{\partial \rho_{mon}}\right]_\beta$ derivative reads

$$\left[\frac{\partial X_0}{\partial \rho_{mon}}\right]_\beta = \left[\frac{\partial X_0}{\partial \Gamma}\right]_{\rho_m\beta}\left[\frac{\partial \Gamma}{\partial \rho_{mon}}\right]_\beta + \left[\frac{\partial X_0}{\partial \rho_{mon}}\right]_{\Gamma\beta}, \tag{4.30}$$

with

$$\left[\frac{\partial X_0}{\partial \Gamma}\right]_{\rho_m\beta} = -\frac{2\Delta\xi}{\pi\sigma}X_0 - \eta\left[\frac{\partial \Delta_1}{\partial \Gamma}\right]_{\rho_m\beta} - \frac{2\Delta\xi}{\pi}\left[\frac{\partial \eta^B}{\partial \Gamma}\right]_{\rho_m\beta}, \tag{4.31}$$

$\left[\frac{\partial X_0}{\partial \rho_{mon}}\right]_{\Gamma\beta}$ defined by (4.21), $\left[\frac{\partial \Delta_1}{\partial \Gamma}\right]_{\rho_m\beta}$ and $\left[\frac{\partial \eta^B}{\partial \Gamma}\right]_{\rho_m\beta}$ given in the Appendix and $\left[\frac{\partial \Gamma}{\partial \rho_{mon}}\right]_\beta$ obtained differentiating equation (4.5) with respect to ρ_{mon}:

$$\begin{aligned}&\left\{1 - \frac{4\pi K\rho_{mon}X_0^2}{(2\Gamma+z)\,\sigma^3}\left(\frac{\Delta\xi}{\pi}\right)^2 + \frac{2\pi K\rho_{mon}X_0}{2\Gamma+z}\Big(1+\right.\\ &\left.+\frac{2\Delta\xi}{\pi\sigma^2}\Big)\left[\frac{\partial X_0}{\partial \Gamma}\right]_{\rho_m\beta}\right\}\left[\frac{\partial \Gamma}{\partial \rho_{mon}}\right]_\beta = \\ &= -\frac{KX_0}{2\Gamma+z}\left(1+\frac{2\Delta\xi}{\pi\sigma^2}\right)\left\{\pi X_0 + 2\pi\rho_{mon}\left[\frac{\partial X_0}{\partial \rho_{mon}}\right]_{\Gamma\beta}\right\}.\end{aligned} \tag{4.32}$$

Now one can easily see that our model, treated in the frames of the TPTD, belongs to the family of the so-called truncatable free energy models [30], since its thermodynamical properties are defined by the finite number of the chain length distribution function moments, i.e. by ρ and ρ_{mon}. This feature allows us to use a scheme developed earlier [1,31] and to map the phase equilibrium conditions for the model at hand onto a set of nonlinear algebraic equations for these moments. As a result the full phase diagram of the model, including cloud and shadow curves, binodals and chain-length distribution functions of the coexisting phases can be calculated. Since this scheme is very similar to that, used in our previous study [1], we will not present it here and proceed to the discussion of the numerical results. For the details we refer the readers to the original publication.

5. Results and discussion

To illustrate our theory we present here numerical results for the phase behavior of polydisperse Yukawa hard-sphere chain mixture with Yukawa

screening parameter $z\sigma = 1.8$ and species distributed according to the distribution function $f^{(0)}(m)$,

$$f^{(0)}(m) = F^{(0)}(m)/\sum_m F^{(0)}(m), \tag{5.1}$$

where for $F^{(0)}(m)$ we have chosen Beta distribution

$$F^{(0)}(m) = \frac{1}{B(\alpha,\beta)}\left(\frac{m}{M}\right)^{\alpha-1}\left(1-\frac{m}{M}\right)^{\beta-1}, \tag{5.2}$$

$m = 1..M$ is the chain length (and species index), $B(\alpha,\beta)$ is the beta function, α and β are related to the mean chain length $\langle m\rangle^{(0)} = \sum_m m f^{(0)}(m)$ and the mean square chain length $\langle m^2\rangle^{(0)} = \sum_m m^2 f^{(0)}(m)$ by

$$\alpha = \frac{M - \langle m\rangle^{(0)}\left(1+D^{(0)}_{\langle m\rangle}\right)}{MD^{(0)}_{\langle m\rangle}}, \qquad \beta = \left(\frac{M-\langle m\rangle^{(0)}}{\langle m\rangle^{(0)}}\right)\alpha \tag{5.3}$$

and $D^{(0)}_{\langle m\rangle} = \langle m^2\rangle^{(0)}/\left(\langle m\rangle^{(0)}\right)^2 - 1$. The distribution function $f^{(0)}(m)$ is normalized, i.e.

$$\sum_m f^{(0)}(m) = 1 \tag{5.4}$$

and the number density of the chains of the length m is $\rho^{(0)}_m = \rho^{(0)} f^{(0)}(m)$, where $\rho^{(0)}$ is the overall number density of the system. Our distribution function is characterized by the average chain length $\langle m\rangle^{(0)} = 8$, maximal chain length $M = 100$ and polydispersity parameter $D^{(0)}_{\langle m\rangle} = 0.5$. At a sufficiently high temperature the mixture is stable as a single phase, called the parent phase. As the temperature is decreased this phase will separate into two daughter phases with the number densities $\rho^{(1)}$ and $\rho^{(2)}$ and chain length distribution functions $f^{(1)}(m)$ and $f^{(2)}(m)$.

In Fig. 1 we show the phase diagram of the system in the (T^* vs $\rho^* = \rho\sigma^3$) (Fig. 1a) and (T^* vs $\eta = \pi\rho^*/6$) (Fig. 1b) planes, calculated using the present TPTD approach and recently developed HTA approach [1]. It contains the cloud and shadow curves and the critical binodals. The cloud curve represents the terminal points of the phase with the density equal to the parent phase density $\rho^{(0)}$ and the shadow curve consists of the points in equilibrium with the corresponding cloud-curve points. Thus the cloud and shadow curves form an envelope for the binodals.

Critical binodal, cloud and shadow curves intersect at the critical point. For the critical point we find $T_{cr}^{*(TPTD)} = 2.729$ ($T_{cr}^{*(HTA)} = 2.676$) and $\rho_{cr}^{*(TPTD)} = 0.0219$ ($\rho_{cr}^{*(HTA)} = 0.0270$). For the reference we have added the phase coexistence curves for a one-component fluid with the chains of the fixed chain length $m = 8$, treated as well in the TPTD and HTA. In the one-component case we have: $T_{cr}^{*(TPTD)} = 2.48$ ($T_{cr}^{*(HTA)} = 2.531$) and $\rho_{cr}^{*(TPTD)} = 0.0226$ ($\rho_{cr}^{*(HTA)} = 0.0266$). The comparison of the phase diagrams for monodisperse and polydisperse versions of the model shows that polydispersity extends the region of the phase instability , shifting the critical point to a higher temperature and slightly lower density. More detailed information on this effect can be extracted from Fig. 2, where position of the critical point at different values of the polydispersity parameter σ_m is presented. We observe that TPTD predicts higher critical temperature and lower critical density in comparison with HTA predictions (Fig. 1). At the same time TPTD critical temperature for the monodisperse case is lower than corresponding HTA critical temperature. Thus, in comparison with HTA TPTD predicts larger critical temperature shift caused by the polydispersity of the system. Since in the one-component case TPTD appears to be more accurate then SAFT-VR [10], which in turn is more accurate then the first-order perturbation theory [6] (which is equivalent to our HTA), we expect that similar holds in the case of polydisperse system, i.e. TPTD gives more accurate predictions then HTA. However this conclusion has to be verified by the comparison of the theoretical predictions with corresponding computer simulation predictions. We find that the overall shape of the phase diagrams, obtained using both theories, are similar to those found in the case of polydisperse mixture of Yukawa hard spheres [1, 32], except that the shadow curves are more narrow and the density of the liquid branch of the shadow phase is lower then the density of the gas branch. However from Fig. 1b, where we present the phase diagrams in the (T^* vs η) plane, we observe that both cloud and shadow curves have the usual symmetric shape. Thus, while the densities of both gas and liquid branches of the shadow phase are close (see Fig. 1a), according to Fig. 1b their packing fractions are rather different and the packing fraction of the liquid branch is higher then that of the gas branch. This is the consequence of the fractionation effects, which cause the long chain particles to move to the liquid phase and the short chain particles to move to the gas phase.

More specific information about the composition of the coexisting phases can be extracted from the distribution functions of the two daughter phases, which give evidence of the effects of fractionation. For the

points located on the cloud and shadow curves and on the binodal at two selected values of the temperature $T^* = 2.0,\ 2.5$, the daughter distribution functions, $f^{(1)}(m)$ and $f^{(2)}(m)$, along with the parent distribution function $f^{(0)}(m)$, are shown in Figs 4 and 3. Distribution functions for the two pairs of points located on the critical binodal at $T^* = 2.0,\ 2.5$ (Fig. 3) show a moderate fractionation effects and a preference for the longer chain particles for the liquid phase and shorter chain particles for the gas phase. This effect becomes more pronounced with the temperature decrease. In Fig.4 we show the distribution functions for the points located on the shadow curve. In these points the system is in equilibrium with the system in the points located either on the liquid branch or on the gas branch of the cloud curve. Here we find a substantial shift of the distribution function maximum towards the longer chain particles in the case of the liquid branch. In the case of the gas branch the corresponding shift in the direction of the shorter chains is smaller but the distribution function substantially sharpens and forms a peak in the region of shortest chains. As the temperature decreases these shifts become stronger and distribution functions become narrower. Quantitative insight into the fractionation effects can be extracted from the analysis of the behavior of the mean chain length $\langle m \rangle$ and mean chain length deviation $\sigma_m = \sqrt{\langle (m - \langle m \rangle)^2 \rangle}$ in the coexisting phases. These quantities along the critical binodal curve and along the shadow curve are plotted in Figs. 5 and 6. As the temperature decreases we see on the shadow curve a strong increase of the mean chain length in the fluid phase and small decrease in the gas phase. Corresponding changes of $\langle m \rangle$ along the liquid branch of the critical binodal is much less pronounced and the mean chain length here is only about two times larger then its counterpart in the gas phase, which is almost coinciding with the mean chain on the gas branch of the shadow curve. From the σ_m curves we learn that the width of the distribution function on the gas branch of the shadow curve decreases with the temperature decrease. Along the liquid branch of the shadow curve σ_m first increases as the temperature decreases up to $T^* \approx 2.5$. Further decrease of the temperature causes the distribution function to decrease its width. Corresponding changes of the distribution function width along the critical binodal are similar to those of the average chain length $\langle m \rangle$ with σ_m on the liquid branch being only about twice larger in comparison with its value on the gas branch.

In summary, our analysis shows, that the longer chain particles prefer the liquid phase and shorter chain particles are predominantly encountered in the gas phase. This behavior is in qualitative agreement with the

experimental results for the fractionation effects in polydisperse polymer mixture in a single solvent [33]. In Figs. 7 and 8 we present a comparison of the theoretical and experimental results for the molecular weight distribution function and for the mean chain length $\langle m\rangle$ and mean square chain length $\langle m^2\rangle$ in the coexisting phases of the polydisperse polymers in a solvent, represented by the polystyrene+methylcyclohexane mixture [33]. We assume that the polymer chain length m is proportional to its molecular weight M_m. Otherwise we have not been making any attempts to fit the model parameters to reproduce the properties of the real system. However we find a reasonable qualitative agreement between the theory and experiment. Both theory and experiment predict that the maxima of the distribution functions, $\langle m\rangle$ and $\langle m^2\rangle$ in the liquid and in the gas phases are shifted in the direction towards the longer and shorter chains, respectively. At the same time we observe, that the maximum of the experimental distribution function in the liquid phase is higher and the maximum of the theoretical distribution function is lower then the corresponding parent distribution functions maxima. Note, however, that experimental distribution functions are not normalized and upon their normalization the liquid phase maximum will became lower and the gas phase maximum will became higher. Thus, both theory and experiment predict that upon phase separation longer polymers equilibrate to the liquid phase and shorter polymers are predominantly encountered in the gas phase.

6. Concluding remarks

In this paper we propose extension of the TPTD for the polydisperse mixture of the hard-sphere Yukawa chain fluid with chain length polydispersity. It is demonstrated that in the frames of the TPTD the model belongs to the class of the so-called truncatable free energy models with thermodynamical properties defined by the finite number of the chain length distribution function moments. This feature enables one to map the phase coexistence relations for the model at hand onto a coupled set of algebraic equations for these moments. We derive explicit analytical expressions for the Helmholtz free energy, chemical potential and pressure in terms of the two distribution function moments. These expressions are used to calculate the full liquid-gas phase diagram, including critical binodal, cloud and shadow curves and distribution functions of the coexisting phases. Comparison of the theoretical results for the distribution functions, mean chain length and mean square chain length with corresponding experimental results, carried out for the polydisperse

polymer mixture in a single solvent [33], shows reasonable qualitative agreement. We have analyzed the behavior of the distribution functions and their first two moments at different temperatures along the critical binodal and shadow curves. According to our analysis and in agreement with experimental findings the longer chain particles prefer to move to the liquid phase and shorter chain particles are predominantly encountered in the gas phase.

A. Γ derivatives

$$\left[\frac{\partial\eta^B}{\partial\Gamma}\right]_{\rho_m\beta} S = \left\{\left[\frac{\partial\Theta^\lambda}{\partial\Gamma}\right]_{\rho_m\beta} + \Delta_1\left[\frac{\partial\Theta^\eta}{\partial\Gamma}\right]_{\rho_m\beta} + \frac{2\Delta\eta^B}{\pi}\left[\frac{\partial\Theta^\xi}{\partial\Gamma}\right]_{\rho_m\beta}\right\}\left(\frac{z^2}{2}+\frac{\pi}{\Delta}\Omega^\eta\right) - \Theta^\eta\left[2\eta^B + \frac{\pi}{\Delta}\left[\frac{\partial\Omega^\lambda}{\partial\Gamma}\right]_{\rho_m\beta} + \frac{\pi}{\Delta}\Delta_1\left[\frac{\partial\Omega^\eta}{\partial\Gamma}\right]_{\rho_m\beta} + 2\eta^B\left[\frac{\partial\Omega^\xi}{\partial\Gamma}\right]_{\rho_m\beta}\right] \tag{1.1}$$

$$\left[\frac{\partial\Delta_1}{\partial\Gamma}\right]_{\rho_m\beta} S = -\frac{2\Delta}{\pi}\left(1-\Theta^\xi\right)\left\{2\eta^B + \frac{\pi}{\Delta}\left[\frac{\partial\Omega^\lambda}{\partial\Gamma}\right]_{\rho_m\beta} + \Delta_1\frac{\pi}{\Delta}\left[\frac{\partial\Omega^\eta}{\partial\Gamma}\right]_{\rho_m\beta} + 2\eta^B\left[\frac{\partial\Omega^\xi}{\partial\Gamma}\right]_{\rho_m\beta}\right\} - \left(2\Gamma + \frac{\pi\rho_{mon}\sigma^2}{\Delta} + z + 2\Omega^\xi\right)\left[\left[\frac{\partial\Theta^\lambda}{\partial\Gamma}\right]_{\rho_m\beta} + \Delta_1\left[\frac{\partial\Theta^\eta}{\partial\Gamma}\right]_{\rho_m\beta} + \frac{2\Delta\eta^B}{\pi}\left[\frac{\partial\Theta^\xi}{\partial\Gamma}\right]_{\rho_m\beta}\right] \tag{1.2}$$

where

$$\left[\frac{\partial\Theta^y}{\partial\Gamma}\right]_{\rho_m\beta} = \frac{2\xi y\Delta}{\pi}\left(\frac{2\xi\Delta}{\pi\sigma^2}+1\right)\rho_{mon}, \tag{1.3}$$

$$\left[\frac{\partial\Omega^y}{\partial\Gamma}\right]_{\rho_m\beta} = \frac{2\xi y\Delta}{\pi\sigma}\left(\frac{2\xi\Delta}{\pi\sigma^2}+\frac{1}{2}\right)\rho_{mon}, \tag{1.4}$$

$$S = \Theta^\eta\left(2\Gamma + \frac{\pi}{\Delta}\zeta_2 + z + 2\Omega^\xi\right) + \frac{\Delta}{\pi}\left(z^2 + \frac{2\pi}{\Delta}\Omega^\eta\right)\left(1-\Theta^\xi\right). \tag{1.5}$$

In above expressions y can take values ξ,η or λ.

$$\left[\frac{\partial y}{\partial\Gamma}\right]_{\rho_m\beta} = -\frac{2\Delta}{\pi\sigma}\xi y. \tag{1.6}$$

B. The ρ_{mon} derivatives

$$\left[\frac{\partial\eta^B}{\partial\rho_{mon}}\right]_{\Gamma,\beta} S = -\left(\frac{\pi\sigma^3}{6\Delta}\Theta^X + \frac{\Theta^X}{\rho_{mon}}\right)\left[\frac{z^2}{2} + \frac{\pi}{\Delta}\Omega^\eta\right] \tag{2.1}$$
$$-\Theta^\eta\left\{2\eta^B\left(\frac{\pi^2\rho_{mon}\sigma^5}{12\Delta^2} + \frac{\pi\sigma^2}{2\Delta}\right) - \frac{\pi^2\sigma^3}{6\Delta^2}\Omega^X - \frac{\pi}{\Delta}\frac{\Omega^X}{\rho_{mon}}\right\}$$
$$\left[\frac{\partial\Delta_1}{\partial\rho_{mon}}\right]_{\Gamma,\beta} S = -\left[2\Omega^\xi + 2\Gamma + z + \frac{\pi\zeta_2}{\Delta}\right]\left(\frac{\pi\sigma^3}{6\Delta}\Theta^X + \frac{\Theta^X}{\rho_{mon}}\right) \tag{2.2}$$
$$-2\left(1-\Theta^\xi\right)\eta^B\left\{\frac{\pi^2\rho_{mon}\sigma^3}{6\Delta} + \sigma^2\right\} + \frac{\pi\sigma^3}{3\Delta}\Omega^X\left(1-\Theta^\xi\right) - \frac{\pi}{\Delta}\frac{\Omega^X}{\rho_{mon}},$$

where S is given by (1.5), Θ^X and Ω^X are found from (4.9) with y replaced by X_0:

$$\frac{\Theta^X}{\rho_{mon}} = -\sigma\left(1 + \frac{\Delta\xi}{\pi\sigma^2}\right)X_0, \quad \frac{\Omega^X}{\rho_{mon}} = -\left(\frac{1}{2} + \frac{\Delta\xi}{\pi\sigma^2}\right)X_0. \tag{2.3}$$

Література

1. S. P. Hlushak and Yu. V. Kalyuzhnyi, *Chem. Phys. Letters* **285**, 285(2007).
2. S. P. Hlushak and Yu. V. Kalyuzhnyi, *J. Phys. Stud.* **11**, 1(2007).
3. A. Gil-Villegas, A. Galindo, P. J. Whitehead, S. J. Mills, G. Jackson, and A. N. Burgess, *J. Chem. Phys.* **106**, 4168(1997).
4. M. S. Wertheim, *J. Stat. Phys.* **42**, 459;477(1986).
5. M. S. Wertheim, *J. Chem. Phys.* **87**, 7323(1987).
6. X. Y. Wang, Y. C. Chiew, *J. Chem. Phys.* **115**, 4376(2001).
7. Yu. V. Kalyuzhnyi, C.-T. Lin, G. Stell, A. Yethiraj, *J Mol. Liq.* **92**, 85(2001).
8. C. McCabe, Yu. V. Kalyuzhnyi, P. T. Cummings, Fluid Phase Eq. **194**, 185(2002).
9. Yu. V. Kalyuzhnyi, C. McCabe, P. T. Cummings, G. Stell, *Mol. Phys.* **100**, 2499(2002).
10. Yu. V. Kalyuzhnyi, C. McCabe, E. Whitebay, P. T. Cummings, *J. Chem. Phys.* **121**, 8128(2004)
11. Y. C. Chiew, *Mol. Phys.* **73**, 359(1991).
12. Yu. V. Kalyuzhnyi, *Mol. Phys.* **94**, 735(1998).
13. Yu. V. Kalyuzhnyi and P. T. Cummings, *J. Chem. Phys.* **103**, 3265(1995).
14. Yu. V. Kalyuzhnyi, C.-T. Lin, and G. Stell, *J. Chem. Phys.* **106**, 1940(1997).
15. C.-T. Lin, Yu. V. Kalyuzhnyi, and G. Stell, *J. Chem. Phys.* **108**, 6513(1998).
16. Yu. V. Kalyuzhnyi, C.-T. Lin, and G. Stell, *J. Chem. Phys.* **108**, 6525(1998).
17. M. S. Wertheim, *J. Stat. Phys.* **35**, 19;35(1984).
18. D. Ghonasgi, W. G. Chapman, *J. Chem. Phys.* **100**, 6633(1994).
19. J. Chang, S. I. Sandler, *Chem. Eng. Sci.* **49**, 2777(1994).
20. P. J. Rossky, R. A. Chiles, *Mol. Phys.* **51**, 661(1984).
21. Yu. V. Kalyuzhnyi, P. T. Cummings, *J. Chem. Phys.* **104**, 3325(1996).
22. M. F. Holovko, Yu. V. Kalyuzhnyi, *Mol. Phys.* **73**, 1145(1991).
23. Yu. V. Kalyuzhnyi, M. F. Holovko, *Mol. Phys.* **80**, 1165(1993).
24. Yu. V. Kalyuzhnyi, P. T. Cummings, *Mol. Phys.* **87**, 249(1996).
25. Yu. V. Kalyuzhnyi, L. Blum, J. Rescic, G. Stell, *J. Chem. Phys.* **112**, 2843(2000).
26. S. P. Hlushak, Yu. V. Kalyuzhnyi, arXiv:0805.0688v1 [cond-mat.soft] (2008); *J. Chem. Phys.*(in preparation).

27. M. Ginoza, *J. Phys. Soc. Japan* **55**, 95(1986).
28. N. F. Carnahan and K. E. Starling, *J. Chem. Phys.* **51**, 635(1969).
29. J. S. Høye and G. Stell, *J. Chem. Phys.* **67**, 439(1977).
30. P. Sollich, *J. Phys.: Condens. Matter* **14**, R79(2002).
31. L. Bellier-Castella, H. Xu, M. Baus, *J. Chem. Phys.* **113**, 8337(2000).
32. Yu. V. Kalyuzhnyi, G. Kahl, *J. Chem. Phys.* **119**, 7335(2003).
33. R. S. Shresth, R. C. McDonald, *J. Chem. Phys.* **117**, 9037(2002).

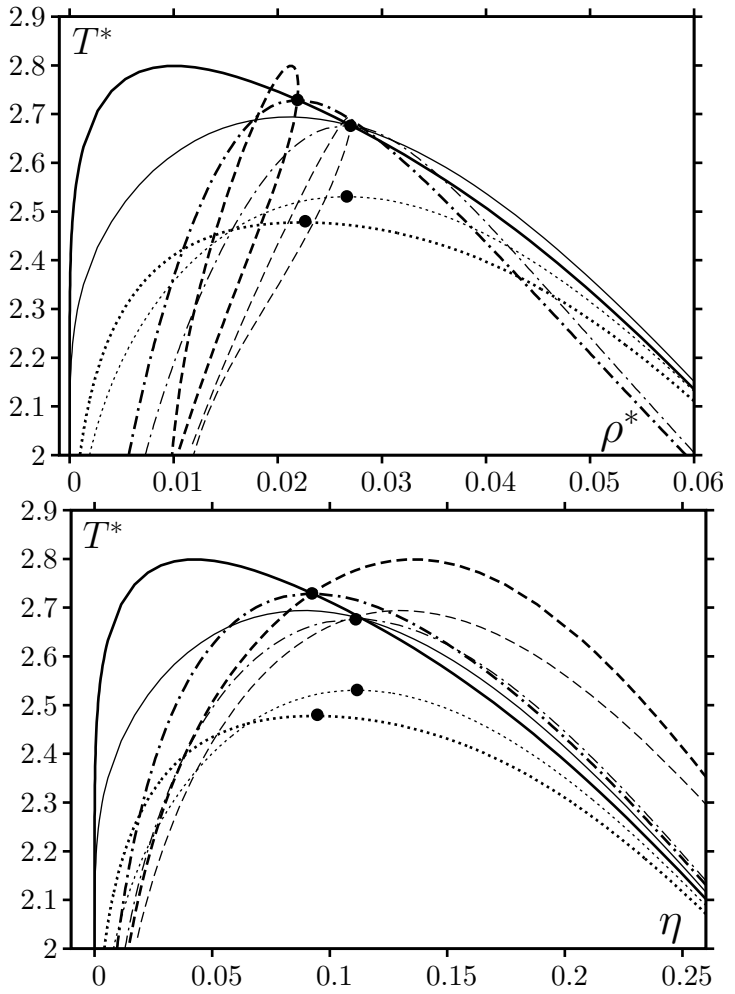

Рис. 1. Phase diagram of polydisperse hard-sphere Yukawa chain mixture with chain length polydispersity in T^* vs ρ^* (upper panel) and T^* vs η (lower panel) coordinate planes. Here TPTD and HTA results are represented by the thick and thin lines, respectively, with cloud and shadow curves plotted by the solid and dashed lines, respectively, critical binodals by the dashed-dotted lines and binodals for monodisperse version of the model by dotted lines. Critical points are denoted by filled circles.

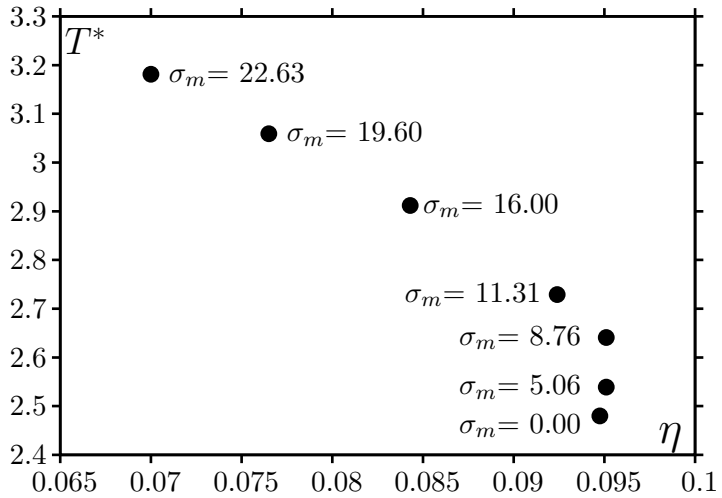

Рис. 2. Position of the critical point on T^* vs η plane (filled circles) at different values of the mean chain length deviation $\sigma_m = \sqrt{\langle (m - \langle m \rangle)^2 \rangle}$.

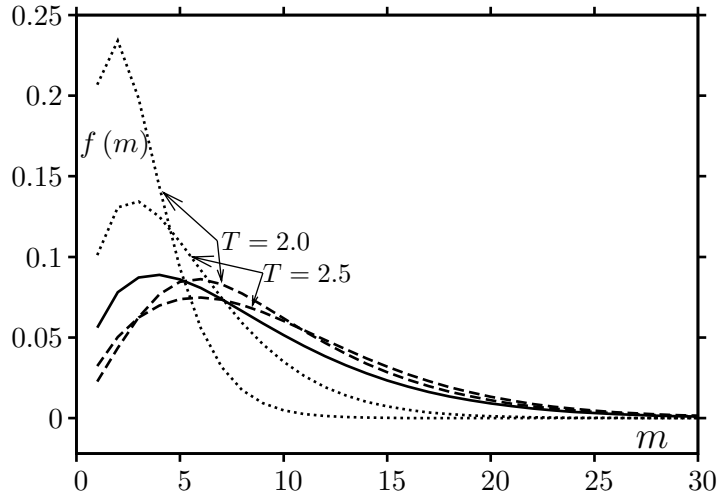

Рис. 3. Distribution functions of the parent phase (solid line) and coexisting gas (dotted lines) and liquid (dashed lines) phases on the critical binodal at $T^* = 2.0,\ 2.5$.

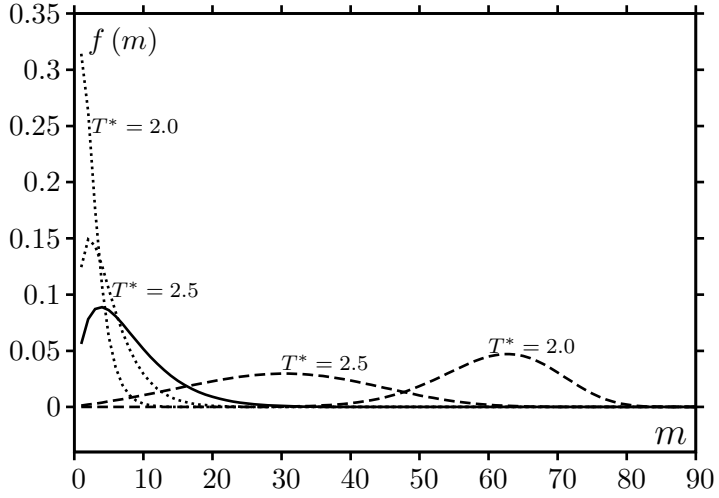

Рис. 4. Distribution functions of the parent phase (solid line) and gas (dotted line) and liquid (dashed lines) daughter phases on the shadow curve at $T^* = 2.0,\ 2.5$.

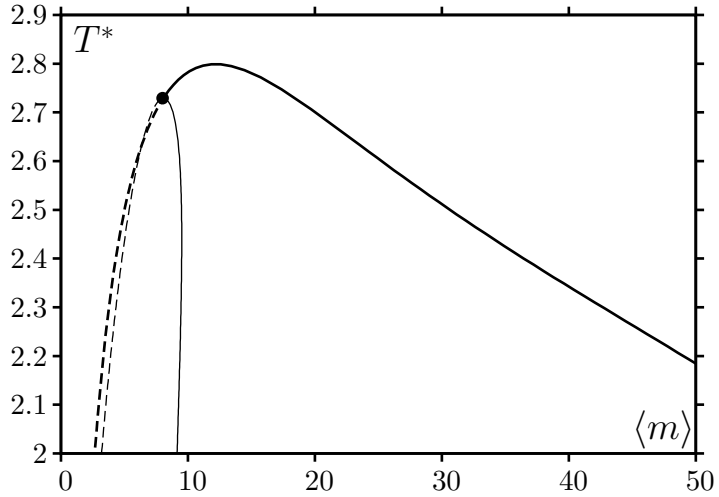

Рис. 5. Average chain length $\langle m \rangle$ along the shadow curve (thick solid and dashed lines) and along the critical binodal (thin solid and dashed lines). Liquid phases are denoted by the solid lines and gas phases are denoted by the dashed lines.

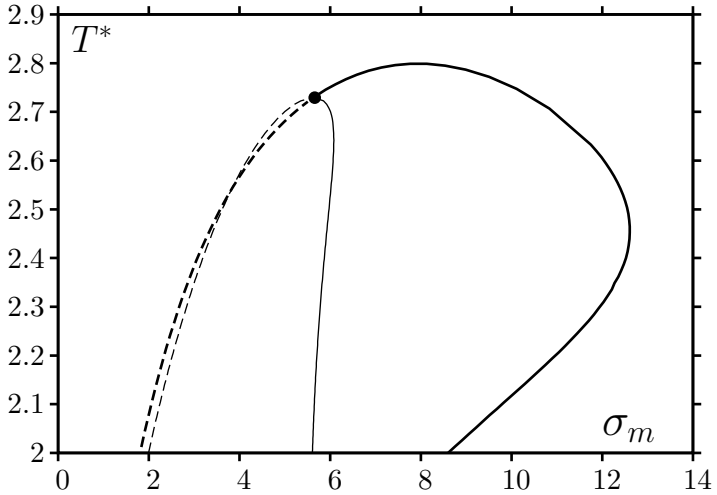

Рис. 6. Mean chain length deviation $\sigma_m = \sqrt{\langle (m - \langle m \rangle)^2 \rangle}$ along the shadow curve (thick solid and dashed lines) and along the critical binodal (thin solid and dashed lines). Liquid phases are denoted by the solid lines and gas phases are denoted by the dashed lines.

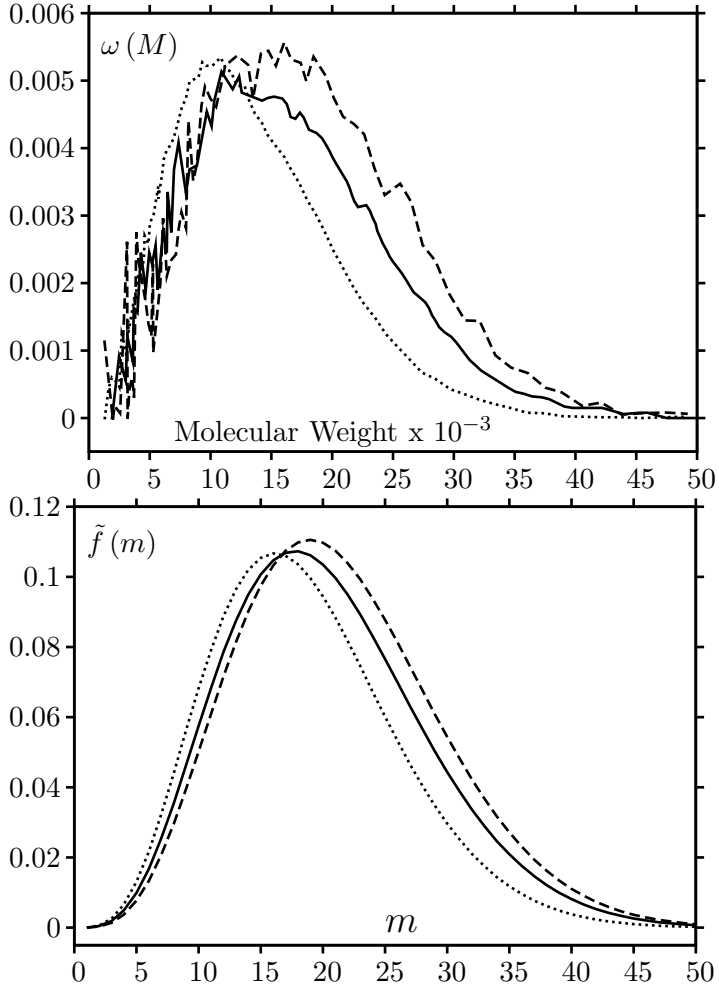

Рис. 7. Weight fraction molecular weight distribution $\omega(M)$ of the polystyrene+methylcyclohexane mixture for the parent phase (solid line) and lower (dashed line) and upper (dotted line) daughter phases [33] and chain length distribution function $\tilde{f}(m) = mf(m)/\langle m \rangle$ of the hard-sphere Yukawa chain mixture for the parent phase (solid line) and liquid (dashed line) and gas (dotted line) daughter phases on the experimental (upper panel) and theoretical (lower panel) critical binodals at $T/T_{cr} = 0.984$, where T_{cr} is either experimental or theoretical critical temperature. Theoretical calculations are carried out for the parent distribution function with $\langle m \rangle^{(0)} = 17$ and $D_{\langle m \rangle} = 0.2$.

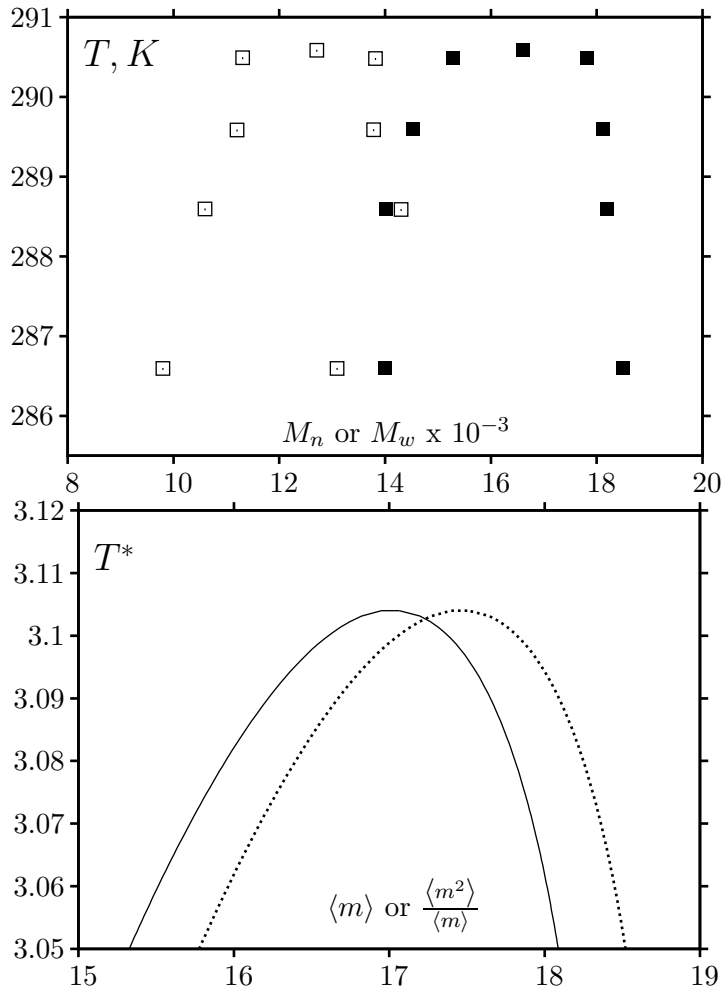

Рис. 8. Number average molecular weight M_n (open squares) and weight average molecular weight M_w (filled squares) of the polystyrene+methylcyclohexane mixture and mean chain length $\langle m\rangle$ (solid line) and mean square chain length $\langle m^2\rangle/\langle m\rangle$ (dotted line) of the hard-sphere Yukawa chain mixture for the coexisting daughter phases on the experimental (upper panel) and theoretical (lower panel) critical binodals. Theoretical calculations are carried out for the parent distribution function with $\langle m\rangle^{(0)} = 17$ and $D_{\langle m\rangle} = 0.2$.

CONDENSED MATTER PHYSICS

The journal **Condensed Matter Physics** is founded in 1993 and published by Institute for Condensed Matter Physics of the National Academy of Sciences of Ukraine.

AIMS AND SCOPE: The journal **Condensed Matter Physics** contains research and review articles in the field of statistical mechanics and condensed matter theory. The main attention is paid to physics of solid, liquid and amorphous systems, phase equilibria and phase transitions, thermal, structural, electric, magnetic and optical properties of condensed matter. Condensed Matter Physics is published quarterly.

ABSTRACTED/INDEXED IN:

- Chemical Abstract Service, Current Contents/Physical, Chemical&Earth Sciences
- ISI Science Citation Index-Expanded, ISI Alrting Services
- INSPEC
- Elsevier Bibliographic Databases (EMBASE, EMNursing, Compendex, GEOBASE, Scopus)
- "Referativnyi Zhurnal"
- "Dzherelo"

CONTACT INFORMATION:
Institute for Condensed Matter Physics
of the National Academy of Sciences of Ukraine
1 Svientsitskii Str., 79011 Lviv, Ukraine
Tel: +38(032)2760908; Fax: +38(032)2761978
E-mail: cmp@icmp.lviv.ua http://www.icmp.lviv.ua